RF-TEST OF A 324-MHz, 3-MeV, H^- RFQ STABILIZED WITH PISL'S

A. Ueno, Y. Kondo, KEK, Tsukuba 305-0801, Japan

Abstract

A 324-MHz, 3.115-m long, four-vane-type, radio-frequency quadrupole (RFQ) linac, which will be used as the most upstream accelerating cavity of the KEK/JAERI Joint Project for high-intensity proton accelerator facility, is under development at KEK. It was designed to accelerate a 30-mA H^- beam from 50 keV to 3 MeV with a 3% duty factor. The accelerating field of the RFQ cavity are stabilized against dipole-mode mixing by using 14 pairs of π-mode stabilizing loops (PISL's). The significantly large frequency separation of 23.3 MHz between the accelerating mode and the nearest dipole mode were attained. By tuning the positions of 22 stub-tuners, a uniform accelerating filed distribution within errors of ±0.6% both longitudinally and azimuthally were easily achieved.

1 INTRODUCTION

On 1997, we started to construct a 324-MHz, four-vane-type, radio-frequency quadrupole (RFQ) linac as the most upstream accelerating cavity of the Japan Hadoron Facility (JHF) project [1,2] at KEK. The RFQ was designed to accelerate a 30-mA H^- beam from 50 keV to 3 MeV with a 3% (600 μsx50 Hz) duty factor based upon the experience of a 432-MHz RFQ [3,4,5,6] development for the Japanese Hadron Project (JHP). The π-mode stabilizing loop (PISL) [7] devised to stabilize the JHP-RFQ against the dipole-mode mixing was adopted to the RFQ. The RFQ design code KEKRFQ [8] developed for the JHP-RFQ, which optimizes cell parameters of RFQ's, was used for the beam optics design of the RFQ. The results of the low power rf measurement of the RFQ cavity are described in this paper.

Since the JHF will be amalgamated with a JAERI's neutron science center project into the KEK/JAERI Joint Project for high-intensity proton accelerator facility, the RFQ will be used as the most upstream accelerating cavity of the facility [9,10].

2 EXPERIMENTAL SETUP

In Figs. 1 and 2, schematic drawings of a cross-sectional view of the RFQ cavity and longitudinal views of the four quadrants of the cavity are shown. The diameters of the RFQ cavity, the rod for PISL, the hole bored on the vane for PISL, the stub-tuner (or movable tuner or coupler) and the port for the stub-tuner (or movable tuner or coupler) are 206 mm, 6 mm and 18 mm, 78 mm and 80 mm, respectively. Since the vane-tips were cut by using two-dimensional cutting method with rotating concave cutters, the cross section of the vane-tips have the same shape through the entire length. Except for the radial matching section, the averaged bore radius has also a constant value of 3.7 mm through the entire length for each vane. The vane-tip curvature is 3.293 mm (89% of the average bore radius). As shown in the figures, fourteen pairs of PISL's (seven pairs of horizontal PISL's and seven pairs of vertical PISL's) are installed. The distance between the neighboring horizontal and vertical PISL's are 215 mm (about a quarter of the free-space rf wavelength). There are thirteen spaces on each quadrant between the neighboring horizontal and vertical PISL's. Thirty-eight of the fifty-two spaces are used as ports for sixteen rf-pick-up loop monitors (M), fourteen stub-tuners with slits for vacuum pumping (Tv), six movable stub-tuners (Tm) and two couplers (C). These locations were chosen in order to remove the mixed higher order modes (TE21n- and TE11n-modes) due to machining errors sufficiently and to make the vacuum conductance in the cavity uniform. We also expect the longitudinal field stability by using two couplers for feeding rf power at different longitudinal positions. In Fig. 3, we show schematic drawings of end-plate and both vane-end shapes. The gap between each vane-end and end-plate is 5 mm. The depths of vane-end cuts from the inner surface of the end-plates are 50.8 mm (entrance) and 43.5 mm (exit), respectively. One of four different beads was moved through inside of each quadrant longitudinally in order to measure the field distribution at the positions shown in Fig. 1 by using bead perturbation method. An aluminum column with 10 mm diameter and 10 mm height were used as the bead.

All of the cavity dimensions were determined based upon the MAFIA [11] and SUPERFISH [12] analyses, considering the empirical frequency shift due to machining errors experienced in the development of the JHP-RFQ cavity. At the bead position, the error of the measured frequency shift produced by the bead perturbation due to the bead position error was estimated to be ±0.2% (the coefficient estimated with MAFIA is 0.7%/mm and the bead position error is less than ±0.3 mm). Since the field strength can be approximated as the square root of the frequency shift, the error of field measurement is ±0.1%.

Figures 4 and 5 are the photographs of the inside view the cavity and the general view of the cavity with instruments for bead perturbation measurements.

3 RF MEASUREMENTS

At first, the field distributions in the four quadrants of the accelerating mode were measured by installing fourteen movable stub-tuners with slits (for low power measurements) to Tv-ports and eight movable stub-tuners (for low power measurements) to Tm- and C-ports. All of the low power tuners were set at the design positions (99.5 mm

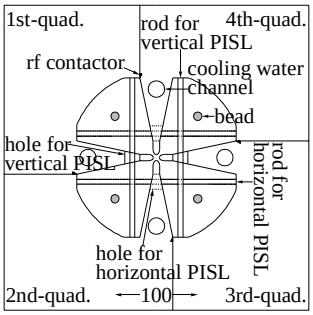

Figure 1: Schematic drawing of cross-sectional shape of the RFQ cavity.

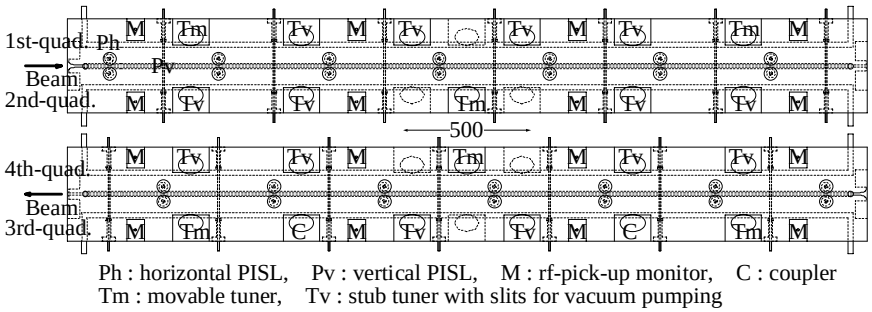

Figure 2: Schematic drawing of longitudinal shape of each quadrant RFQ cavity.

from the beam axis). Sixteen rf-pick-up loop monitors for high power operation were installed to all of M-ports. The measured distributions of the square of field strength are shown in the top graph of Fig. 6. The longitudinal field nonuniformity is speculated to be produced by the modulation effect. The larger modulation is speculated to have the larger capacitance.

The field distribution measurements after slight tuning the positions of the low power tuners were repeated several times iteratively in order to attain the sufficiently uniform field distributions both longitudinally and azimuthally. The measured distributions of the square of field strength are shown in the middle graph of Fig. 6. Since the field strength near the tuner position is locally distorted due to the effect of the tuner itself, the field uniformity was estimated by comparing the field strengths at the M-ports and the remaining fourteen spaces without any ports shown by the arrows (all of the four quadrants at solid arrow and two quadrants at dashed arrow). Since the uniformity of the distributions are less than ±1.1%, the field is distributed within errors of ±0.6% both longitudinally and azimuthally. The stub position extracted from the design position of each tuner according to the measurement was shown in the bottom graph of Fig. 6. During the tuning, four movable end-stub-tuners (for low power measurements) with a diameter of 58 mm (a diameter of the hole for the stub was 60 mm) were also located on each end-plate. The four end-stub-tuners on the entrance end-plate were extracted 1mm and those on exit end-plate were extracted 2 mm, as shown in Fig. 3. The resonant frequency was also tuned to be 323.9 MHz, which is equivalent to the design frequency of 324 MHz in the vacuum. The unloaded Q-value of the cavity was measured to be 8960, which was 79 % of the MAFIA estimation. The frequency of the nearest dipole mode (TE110-mode) was 347.2 MHz.

Finally, instead of the two low power tuners installed at two C-ports, two low power movable couplers with various loop shapes are installed. Thus, the best loop shape and the loop position were determined experimentally for keeping the field uniformity and to attaining sufficient coupling.

4 CONCLUSIONS

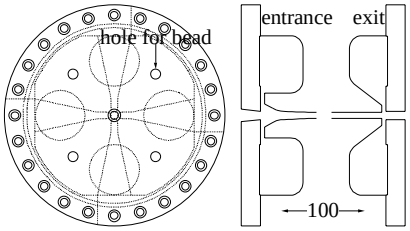

Figure 3: Schematic drawings of end-plate and both vane ends shapes of the RFQ cavity.

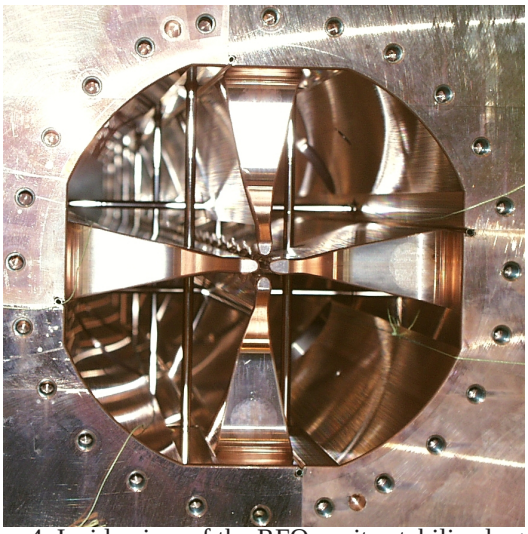

Figure 4: Inside view of the RFQ cavity stabilized against dipole-mode mixing with PISL's.

Figure 5: A photograph of experimental setup for the rf-field measurement.

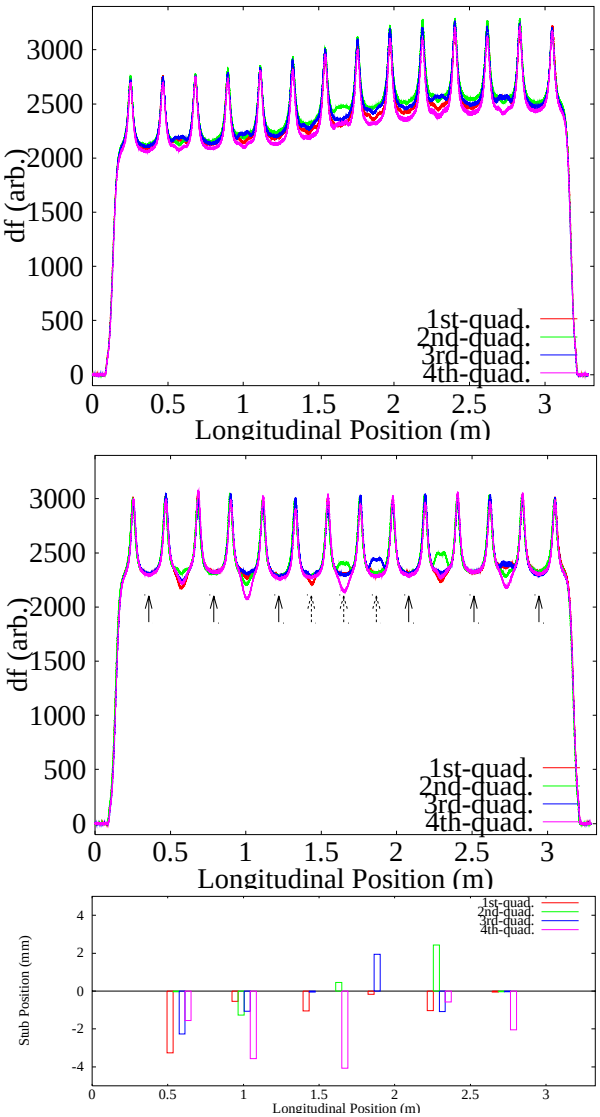

Figure 6: Distributions of the square of field strength in the four quadrants measured with bead perturbation method (top graph: before tuning, middle graph: after tuning *field uniformity <±0.6%) and Each stub position extracted from the design value (bottom figure).

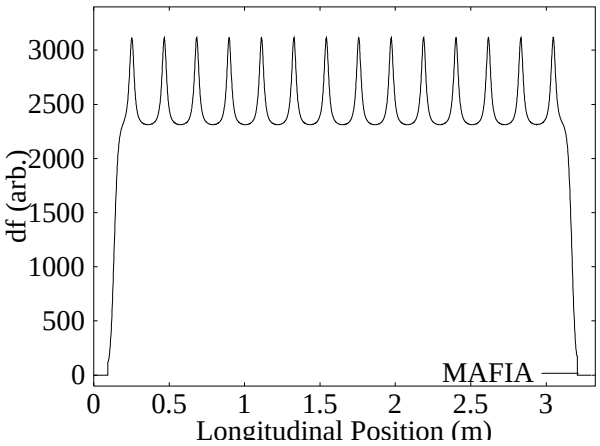

Figure 7: Normalized distribution of the square of field strength at the bead position analyzed with MAFIA.

The low-power rf characteristics of the RFQ stabilized with the PISL's were measured. Fourteen pairs of PISL's installed to the RFQ enlarged the frequency separation between the accelerating mode and the nearest dipole mode from about 5 MHz (estimation) to 23.3 MHz. The field distribution in the four quadrants of the RFQ cavity was measured by the bead-perturbation method. By tuning the positions of 22 stub-tuners, a uniform accelerating filed distribution within a errors of ±0.6% both longitudinally and azimuthally were easily achieved. The distribution showed a good agreement with that analyzed by using MAFIA (shown in Fig.7). The measured Q-value of 8960 was 79% of the calculated value with the MAFIA.

The high power tuners, couplers and end-plates, which have the shapes determined by the low power rf measurements, will be installed into the RFQ cavity. After the low power rf measurement to check the machining errors of these parts, high power rf will be fed to the RFQ cavity in near future.

Acknowledgment

The authors wish to express their sincere thanks to Mr. Kazuyuki Suzuki and the other members of Nuclear Equipment Design Section and Tools Section at Hitachi Works, Hitachi, Ltd. for their technical supports.

REFERENCES

[1] JHF Project Office, KEK Report 97-16, JHF-97-10, 4.4, (1998).
[2] A. Ueno, "200 MeV Linac 4.Ion Source, LEBT and RFQ", The 2nd International Advisory Committee Meeting for JHF Accelerator, (1998).
[3] A. Uneo et al., Proc. 1994 Linear Accelerator Conf., 166, (1994).
[4] A. Uneo et al., Proc. 1994 Linear Accelerator Conf., 169, (1994).
[5] A. Uneo et al., Proc. 1994 Linear Accelerator Conf., 172, (1994).
[6] A. Uneo et al., Proc. 1996 Linear Accelerator Conf., 293, (1996).
[7] A. Ueno and Y. Yamazaki, Nucl. Instr. and Meth. A300, 15, (1991).
[8] A. Ueno and Y. Yamazaki, Proc. 1990 Lin. Accel. Conf., LANL report, LA-12004-C, 329, (1991).
[9] K. Hasegawa et al., "The KEK/JAERI Joint Project: Status of Design and Development", in this conference.
[10] Y. Yamazaki et al., "The Construction of the Low-Energy Front 60-MeV Linac for the JAERI/KEK Joint Project", in this conference.
[11] T. Weiland, Part. Accel., 17, 227, (1985).
[12] K. Halbach et al., Part. Accel. 7, 213, (1976).